THE JOURNAL OF PHYSICAL CHEMISTRY B

Article

pubs.acs.org/JPCB

Interaction Forces, Heteroaggregation, and Deposition Involving Charged Colloidal Particles

Gregor Trefalt,* F. Javier Montes Ruiz-Cabello, and Michal Borkovec

Department of Inorganic and Analytical Chemistry, University of Geneva, Sciences II, 30 Quai Ernest−Ansermet, 1205 Geneva, Switzerland

ABSTRACT: Force profiles as well as aggregation and deposition rates are studied for asymmetrically charged particles and surfaces in aqueous electrolytes theoretically. Interactions are calculated within the Derjaguin, Landau, Verwey, and Overbeek (DLVO) theory, whereby the electrostatic part is modeled at Poisson−Boltzmann (PB) level. Unequally charged surfaces are examined, from the symmetric system, where both surfaces are equally charged, to fully asymmetric systems, where the surfaces are oppositely charged. Charged-neutral systems, where one surface is charged and the other is neutral, emerge as an essential scenario. In this case, the choice of boundary conditions used for solving the PB equation is crucial, whereby constant charge and constant potential boundary conditions lead to either fully repulsive or fully attractive forces. Consequently, charge regulation has a major influence on particle aggregation and deposition rates too. In the charge-neutral case, substantial shifts in the critical coagulation concentration (CCC) are observed when the regulation properties are changed. In the presence of multivalent ions, these systems behave similarly to the symmetrically charged ones. The CCC decreases with the square of the valence in weakly charged systems, while unrealistically high charge densities are needed to recover the classical Schulze−Hardy limit, which predicts a sixth power dependence on valence.

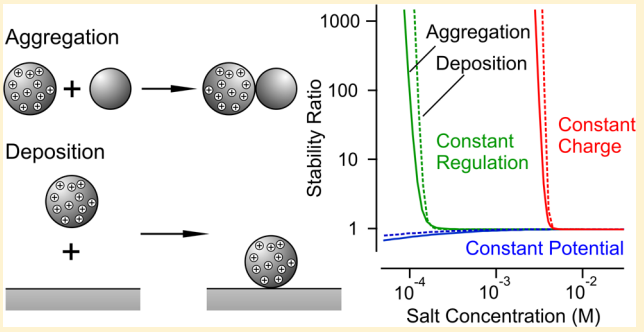

1. INTRODUCTION

Interactions between charged surfaces in aqueous solutions are of substantial importance in material and environmental sciences. Some examples of these applications include paper making,[1,2] ceramic processing,[3−5] wastewater treatment,[6,7] and transport of particles in the subsurface.[8] Physical processes in these applications often include control of particle aggregation or deposition. Therefore, forces between surfaces play a central role in these systems.

Double layer forces between charged surfaces can be often quantitatively described by Poisson−Boltzmann (PB) theory down to distances of a few nanometers.[9−14] When these forces are added to van der Waals forces, one arrives to the theory developed by Derjaguin, Landau, Verwey, and Overbeek (DLVO).[15,16] This theory predicts forces involving particles and surfaces, which are crucial to quantify aggregation and deposition behavior in colloidal systems.[11,17,18]

PB calculations mostly rely on a numerical solution of the underlying nonlinear differential equation.[17,19−21] Analytical solutions are more easily obtained within the Debye−Hückel (DH) approximation, which represents a linearization of the PB theory that is valid only for low electric potentials.[15,22] In real situations, however, this condition may not be satisfied and the full PB approach is needed. Force profiles calculated within PB theory can be sensitive to boundary conditions, especially at small separation distances.[23−25] Normally, constant charge (CC) and constant potential (CP) boundary conditions are used. In general, however, the surfaces may change their surface charge and potential upon approach. This charge regulation phenomenon originates from a shift of the adsorption equilibrium of ions upon approach, and can be treated in a simplified fashion with the constant regulation (CR) approximation.[23−25]

The classical PB theory utilizes the mean-field approximation, which neglects the finite size of the ions and ion−ion correlations. Detailed treatment of all Columbic interactions in electrolyte solutions on the primitive model level reveals that the mean-field PB approach may fail, especially in the presence of multivalent ions.[26−30] In particular, ion−ion correlations may modify effective surface charge and may even induce a charge reversal (overcharging).[13,14,31,32] They can equally induce short-ranged attractive forces between similarly charged surfaces.[30] Nevertheless, PB theory is still valid at larger separations, where the ion−ion correlation and excluded volume effects are small, provided that renormalized or effective surface charge densities or potentials are used.[33,34] These effective quantities can be determined experimentally, for example, by means of electrokinetic techniques[15] or direct force measurements.[35]

Direct force measurements confirm the validity of the PB approach down to distances of a few nanometers, even in the presence of multivalent ions.[9,13,14,19,35,36] In these situations,

Received: April 11, 2014
Revised: May 21, 2014
Published: May 21, 2014

the use of an effective potential is a crucial component, since adsorption of multivalent ions may modify the surface potentials of charged surfaces strongly. Charge regulation effects may be extremely important in such asymmetric systems, especially when one of the particles is almost electrically neutral. In such situations, forces may vary from repulsive to attractive depending on the boundary conditions.[20,37]

Interactions between surfaces also play an important role in particle deposition to substrates. The deposition process consists of two steps, namely, transport toward the surface and particle attachment.[18,22] The first step is mainly governed by convection, while the second by diffusion in the particle−surface force field. The deposition process resembles a limiting case of heteroaggregation, where one of the particles is extremely large.

The kinetics of deposition and heteroaggregation involving oppositely charged surfaces were studied previously.[38−41] The forces in oppositely charged systems were also measured with the colloidal probe technique.[20,36,37,42−44] However, the charged-neutral case, where one particle is charged while the other is neutral, has been addressed only rarely,[20,37] especially in the context of heteroaggregation or deposition. Therefore, we mainly focus on such charged-neutral systems here, and study the corresponding heteroaggregation and deposition behavior in detail. We apply the PB description to the underlying interaction forces. First, we analyze the effect of charge asymmetry, and subsequently the importance of charge regulation effects. We show that these effects may qualitatively change the interactions, and hence dramatically modify the heteroaggregation and deposition behavior in such systems. Lastly, effects of multivalent ions in the charged-neutral system are explored. We find that dependencies on the counterion valence are similar to the case of symmetrically charged particles.

2. THEORY

Interaction free energies are calculated in the plate−plate geometry within DLVO theory and are converted to forces by means of the Derjaguin approximation. From these forces, interaction free energies are obtained, and used for the calculation of heteroaggregation and deposition rates.

Double Layer Interactions. The double layer interactions entering the DLVO theory are calculated in the plate−plate geometry within the Poisson−Boltzmann (PB) model, or by its linearization through the Debye−Hückel (DH) approximation.

Consider two charged plates separated by a distance h immersed in an electrolyte solution containing different types of ions of number concentration c_i and valence z_i. The dependence of the electrostatic potential $\psi(x)$ on the position x, whose origin is taken at the midplane, is governed by the PB equation

$$\frac{d^2\psi}{dx^2} = -\frac{q}{\varepsilon_0\varepsilon}\sum_i z_i c_i e^{-z_i q\psi/(k_B T)} \tag{1}$$

where q is the elementary charge, ε_0 is the dielectric permittivity of the vacuum, ε is the dielectric constant, $k_B T$ is the thermal energy, with k_B being the Boltzmann constant and T the absolute temperature, and the sum runs over all types of ions i. We assume a temperature of 25 °C and use $\varepsilon = 80$ as appropriate for water.

Within the constant regulation (CR) approximation, the solution of the PB equation must be found with the boundary conditions[21]

$$\pm\varepsilon_0\varepsilon\left.\frac{d\psi}{dx}\right|_{x=\pm h/2} = \sigma_\pm - C_I^{(\pm)}[\psi(\pm h/2) - \psi_\pm] \tag{2}$$

where $\sigma_\pm$, $\psi_\pm$, and $C_I^{(\pm)}$ refer to the surface charge density, surface potential, and inner layer capacitance of the isolated surface. The ± signs refer to the right and left surfaces situated at $x = \pm h/2$. This equation represents a Taylor expansion of the charge potential relationship around infinite separation, and its linearization represents the essence of the CR approximation. Instead of the inner layer capacitance, we introduce the regulation parameter defined as

$$p_\pm = \frac{C_D^{(\pm)}}{C_D^{(\pm)} + C_I^{(\pm)}} \tag{3}$$

where the diffuse layer capacitance is obtained from

$$C_D^{(\pm)} = \frac{\partial\sigma_\pm}{\partial\psi_\pm} = \pm\left(\frac{q^2\varepsilon_0\varepsilon}{2k_B T}\right)^{1/2}\frac{\sum_i z_i c_i[e^{-z_i q\psi_\pm/(k_B T)} - 1]}{\{\sum_i c_i[e^{-z_i q\psi_\pm/(k_B T)} - 1]\}^{1/2}} \tag{4}$$

and the diffuse layer potentials $\psi_\pm$ are calculated from the charge−potential relationship

$$\sigma_\pm = \pm\{2k_B T\varepsilon_0\varepsilon\sum_i c_i[e^{-z_i q\psi_\pm/(k_B T)} - 1]\}^{1/2} \tag{5}$$

The ± sign on the left-hand side of the previous two equations refers to positive and negative surface potentials. The regulation parameters quantify the extent of the charge variation of the respective surfaces upon approach. The classical boundary conditions of constant charge (CC) and constant potential (CP) can be recovered by $p_\pm = 1$ and $p_\pm = 0$, respectively. In experimental situations, the regulation parameters between 0 and 1 are typically measured.[13,20,36,37] These results imply that surfaces indeed change the charge upon approach. In the case of extreme charge regulation, $p_\pm \leq 0$ is possible, yielding weaker forces than the CP condition.[45]

When the electrostatic potential profile is known, the swelling pressure follows from

$$\Pi = k_B T\sum_i c_i[e^{-z_i q\psi/(k_B T)} - 1] - \frac{\varepsilon_0\varepsilon}{2}\left(\frac{d\psi}{dx}\right)^2 \tag{6}$$

Integration of the swelling pressure yields the free energy per unit area of the double layer as

$$W_{dl}(h) = \int_h^\infty \Pi(h')\,dh' \tag{7}$$

The linearization of the PB equation yields the DH approximation

$$\frac{d^2\psi}{dx^2} = \kappa^2\psi \tag{8}$$

where κ is the inverse Debye length defined by $\kappa^2 = 2q^2 I/\varepsilon_0\varepsilon k_B T$, where I is the ionic strength given by $I = (1/2)\sum_i z_i^2 c_i$, which is also expressed as a number concentration. Within the DH approximation, the electrolyte composition enters only through the ionic strength. Therefore, electrolytes having the same ionic strength, but eventually different ionic composition, lead to the same results. The linearization is only valid when

dx.doi.org/10.1021/jp503564p | J. Phys. Chem. B 2014, 118, 6346−6355

$|\psi z_{max} q|$ is small with respect to the thermal energy, $k_B T$, where z_{max} is the maximal valence of the ions in the electrolyte solution. Therefore, the validity for 1:1 electrolytes is around 25 mV, but for 1:2 electrolytes, it is at 12 mV.[21] Within the DH approximation, the charge−potential relationship is linear, $\sigma_\pm = \varepsilon_0 \varepsilon \kappa \psi_\pm = C_D \psi_\pm$, where C_D is the diffuse layer capacitance. The solution of the DH equation also depends on the boundary conditions given in eq 2 and the regulation parameter defined in eq 3. Under these conditions, an analytical solution for the electrostatic potential profile between two charged plates can be found.[23] The swelling pressure follows from the low-potential expansion of eq 6

$$\Pi = \frac{\varepsilon_0 \varepsilon}{2}\left[\kappa^2 \psi^2 - \left(\frac{d\psi}{dx}\right)^2\right] \tag{9}$$

and with eq 7 one obtains for the double layer free energy[23]

$$W_{dl}(h) = \varepsilon\varepsilon_0\kappa \frac{2\psi_+\psi_- e^{-\kappa h} + [(2p_+ - 1)\psi_-^2 + (2p_- - 1)\psi_+^2]e^{-2\kappa h}}{1 - (2p_+ - 1)(2p_- - 1)e^{-2\kappa h}} \tag{10}$$

For CP boundary conditions ($p_- = p_+ = 0$), we recover the frequently used relation introduced by Hogg, Healy, and Fuerstenau.[46] The relevant charge-neutral case comprises one charged and another neutral surface, with $\psi_- = 0$. In this case, we obtain

$$W_{dl}(h) = \varepsilon\varepsilon_0\kappa \frac{\psi_+^2(2p_- - 1)e^{-2\kappa h}}{1 - (2p_+ - 1)(2p_- - 1)e^{-2\kappa h}} \tag{11}$$

Here, the sign of the interaction is determined by the regulation parameter of the neutral surfaces. The forces are repulsive for $p_- > 1/2$, and they become attractive for $p_- < 1/2$.

Interaction Forces. The DLVO theory assumes that the interaction free energy per unit area is a sum of van der Waals and electrical double layer contribution

$$W(h) = W_{vdW}(h) + W_{dl}(h) \tag{12}$$

where h is the separation distance. We approximate the van der Waals interaction by neglecting retardation effects with $W_{vdW}(h) = -H/12\pi h^2$, where H is the Hamaker constant.[15]

Interaction forces involving other geometries can be calculated with the Derjaguin approximation $F = 2\pi R_{eff} W(h)$, where R_{eff} is the effective radius given by $R_{eff} = R_+R_-/(R_+ + R_-)$ in the sphere−sphere geometry with R_+ and R_- being the radii of the two spheres.[15] For the sphere-plate geometry, $R_{eff} = R_+$. Integration of the force finally leads to the interaction free energy $V(h)$.

Aggregation Rates. These rates are experimentally accessible through, for example, time-resolved light scattering.[41,47] Treating the diffusion in a force field leads to the aggregation rate coefficient[22]

$$k = \frac{2k_B T}{3\eta R_{eff}}\left[\int_0^\infty \frac{B(h)}{(R_+ + R_- + h)^2} \exp\left(\frac{V(h)}{k_B T}\right) dh\right]^{-1} \tag{13}$$

where $V(h)$ is the interaction free energy between two particles, η the shear viscosity of the fluid, and $B(h)$ the hydrodynamic resistance function. The resistance function can be approximated as[22,48]

$$B(h) = \frac{6(h/2R_{eff})^2 + 13(h/2R_{eff}) + 2}{6(h/2R_{eff})^2 + 4(h/2R_{eff})} \tag{14}$$

The aggregation rate coefficients are often reported as dimensionless stability ratios $W^{(a)} = k_{fast}/k$, where k_{fast} is the aggregation rate coefficient of the reference condition. This condition is normally chosen in the fast aggregation region, where only attractive van der Waals forces are operational.

Deposition Rates. Colloidal particles depositing to spherical collectors can be described within the boundary-layer approximation.[18,22] This approximation implies that the interaction forces between the collector and the particle act on distances small compared to the extension of the diffusion boundary layer. The rate of particle deposition is then obtained from the single collector efficiency $\overline{\eta}$ which is the rate of particle removal by the collector relative to the rate of particle flux toward the collector.[18] Considering particle−collector interaction forces and effects of neighboring collectors on the flow field, one obtains[18]

$$\overline{\eta} = 4.0 A_s^{1/3} Pe^{-2/3}\left(\frac{\beta}{1+\beta}\right) S(\beta) \tag{15}$$

where A_s is a porosity dependent parameter, $Pe = 2R_C u/D$ is the Peclet number, R_C is the radius of the collector, u is the flow velocity, D is the single particle diffusion coefficient far from the collector, and $S(\beta)$ is a slowly varying function.[49] The parameter β is defined as[22]

$$\beta = 1.12 A_s^{-1/3}\left(\frac{DR_C^2}{u}\right)^{1/3} \left\{\int_0^\delta \left[\overline{B}(h)\exp\left(\frac{V(h)}{k_B T}\right) - 1\right] dh\right\}^{-1} \tag{16}$$

where h is the separation distance, δ is the diffusion boundary layer thickness, $\overline{B}(h)$ is the hydrodynamic function, and $V(h)$ is the interaction free energy between particle and collector. The hydrodynamic function can be approximated as $\overline{B}(h) = 1 + R_+/h$, where R_+ is the radius of the depositing particle. The numerical values of this function are similar to eq 14.

Deposition rates are often reported as the relative collision efficiency, which is the ratio between single collector efficiency and single collector efficiency at certain reference conditions. Here we will use the inverse collision efficiency $W^{(d)}$, which is comparable to the stability ratio used in aggregation. This quantity is defined as $W^{(d)} = \overline{\eta}_{fast}/\overline{\eta}$, where $\overline{\eta}_{fast}$ is the collector efficiency at the reference conditions, which are taken under conditions where only van der Waals forces are present.

The upper limit δ of the integral in eq 16 represents the thickness of the diffusion boundary layer.[22] At this distance, the interaction force between particle and collector is negligible, and the result depends only weakly on this value. Since a variation of this limit from 100 nm to 10 μm yields practically the same results, this value was set to 1 μm.

Critical Coagulation Concentration. Repulsive electrostatic interactions at low salt concentrations lead to stable suspensions. When the salt levels are increased, van der Waals interaction dominates and the suspension destabilizes. The transition between stable and unstable suspension is rather sharp and is referred to as the critical coagulation concentration (CCC). A similar transition between slow and fast deposition rate is also observed in deposition experiments. The transition

dx.doi.org/10.1021/jp503564p | J. Phys. Chem. B 2014, 118, 6346−6355

occurs when the energy barrier of the interaction vanishes, mathematically[21]

$$V(h_{max}) = 0 \quad \text{and} \quad \left.\frac{dV}{dh}\right|_{h=h_{max}} = 0 \tag{17}$$

where h_{max} is the separation at the maximum of the interaction potential. Let us apply these conditions to the charge-neutral system. The respective scaling law in the DH limit can be obtained by inserting the respective DH free energies in eq 17. For a symmetric z:z electrolyte, we obtain

$$\text{CCC} \propto \frac{(2p_- - 1)^{2/3}\sigma_+^{4/3}}{z^2} \tag{18}$$

The high-potential PB limit can be obtained by replacing the diffuse layer potential in the DH approximation by the effective potential,[21] and the corresponding high-potential limit becomes

$$\text{CCC} \propto \frac{(2p_- - 1)^2}{z^6} \tag{19}$$

In the charged-neutral system, the $1/z^6$ Schulze–Hardy limit is only reached for extremely high surface charge densities. The symmetric systems behave similarly.[21] In the charged-neutral case, however, the CCC is sensitive to the regulation parameter of the neutral surface. This behavior is in contrast to homoaggregation, where charge regulation plays a minor role.

3. RESULTS AND DISCUSSION

We now discuss interaction forces between unequally charged surfaces and the corresponding stability ratios for hetero-aggregation and deposition. Approximately symmetric systems, where the charge of both surfaces has the same sign and the magnitudes of the surface charge density are comparable, are referred to as *similarly charged* systems. When the particles are unequally charged, we distinguish two cases. In the first case, the sign of the surface charges is opposite, while the surface charge densities are comparable in magnitude. This case is referred to as an *oppositely charged* system. In the second case, one of the surfaces is charged, while the other one is neutral. This case will be referred to as the *charged-neutral* system, and will be discussed in the following.

Our approach is based on the DLVO theory, whereby the PB theory is used to calculate the double layer interactions. Particularly, we study the influence on the asymmetry of the surface charge density of the surfaces on the interactions and the respective stabilities. The main part of the study is focused on the charged-neutral system, where the important role of charge regulation effects is studied. The influence of the electrolyte composition is equally addressed.

Surface Charge Density Asymmetry. We first investigate how the surface charge densities influence the interactions and stability ratios. The interactions between similarly and oppositely charged surfaces were discussed earlier.[36,42−44] In similarly charged systems, the surfaces are repulsive at low salt concentrations, while they become attractive at high concentrations. In oppositely charged systems, the forces are attractive irrespective of the salt concentration. The charged-neutral systems feature more complex behavior, which will be discussed below.[20,37]

Figure 1 illustrates the force profiles in 1:1 electrolytes from similarly charged systems, through charged-neutral systems, to oppositely charged systems. The Hamaker constant $H = 5 \times 10^{-21}$ J is used in the following. This value corresponds to typical values for polystyrene latex particles in aqueous media as measured by the colloidal probe technique.[14,20,50] Normalized forces F/R_{eff} are used, which are independent of the geometry considered. Figure 1a shows the similarly charged system, where $\sigma_+ = \sigma_- = 3$ mC/m^2. Recall that the + and − subscripts denote the surfaces located in the left- and right-hand side from the midplane, respectively. The same subscript will also be used to denote the two particles considered. The first surface charge density is now fixed to $\sigma_+ = 3$ mC/m^2, and the second surface

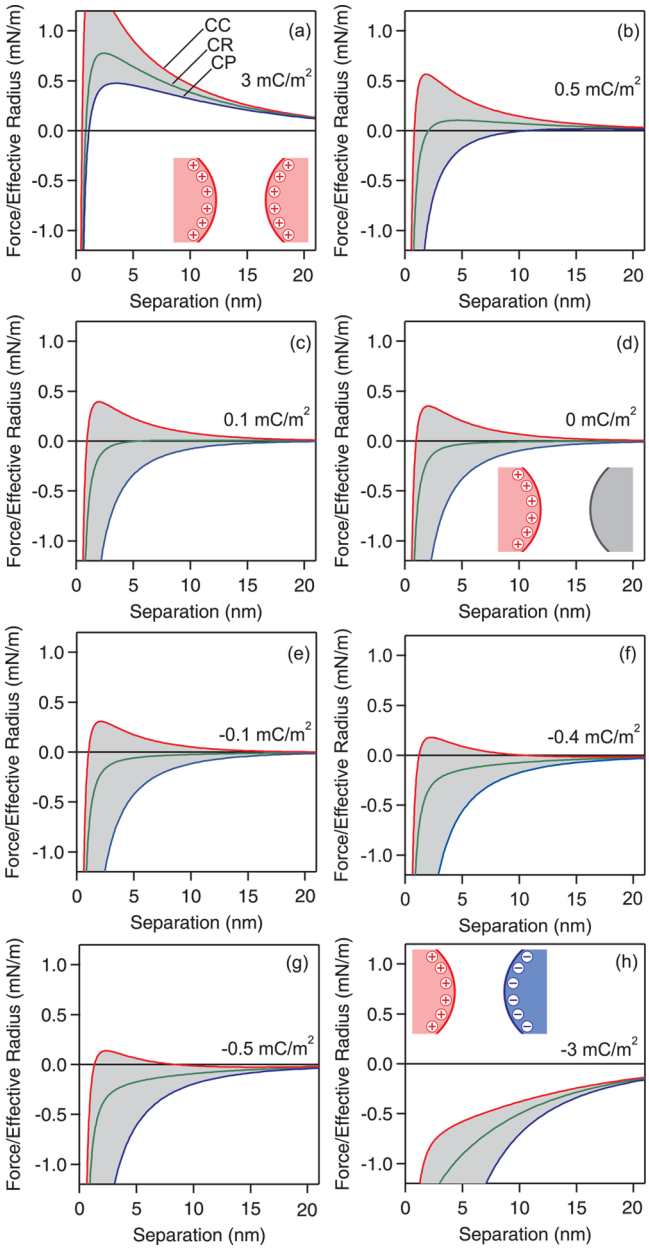

Figure 1. Interaction forces versus the separation distance between two differently charged colloidal particles predicted by DLVO. The PB model with CC, CP, and CR boundary conditions was used. The first particle has a constant surface charge density of $\sigma_+ = 3$ mC/m^2, while the surface charge density of the second particle σ_- changes: (a) 3 mC/m^2, (b) 0.5 mC/m^2, (c) 0.1 mC/m^2, (d) 0 mC/m^2, (e) −0.1 mC/m^2, (f) −0.4 mC/m^2, (g) −0.5 mC/m^2, and (h) −3 mC/m^2. In all cases, the concentration of 1:1 electrolyte is 1 mM, the Hamaker constant is $H = 5 \times 10^{-21}$ J, and for CR boundary conditions the regulation parameters are $p_+ = p_- = 1/2$.

dx.doi.org/10.1021/jp503564p | J. Phys. Chem. B 2014, 118, 6346−6355

charge density is varied from 0.5 to −3 mC/m^2; see Figure 1b–h. Constant charge (CC), constant potential (CP), and constant regulation (CR) boundary conditions with $p_\pm = 1/2$ are compared. The forces between the similarly charged particles are repulsive at large distances due to double layer forces, while at small distances they become attractive, as the van der Waals force prevails. The three boundary conditions all predict qualitatively the same interaction with a pronounced maximum in the force profile. When the charge of the second particle is reduced to 0.5 mC/m^2, the different boundary conditions also predict qualitatively different force profiles. In the CC and CR situations, forces are repulsive in a wide separation range, while the CP condition predicts an attractive force. When the asymmetry of the charge is further increased, the boundary conditions become increasingly important, and they determine whether the double layer interaction is attractive or repulsive. In the charged-neutral system, the CC conditions predict repulsive forces down to separations of a few nanometers, while the force calculated with the CP boundary is attractive; see Figure 1d. In this case, the forces are extremely sensitive to the charge regulation. When the particles are exactly oppositely charged, $\sigma_+ = 3$ mC/m^2 and $\sigma_- = -3$ mC/m^2, the forces are all attractive, and the effect of the charge regulation is weak.

The effects of charge asymmetry and boundary conditions on the heteroaggregation stability ratio in 1:1 electrolyte are presented in Figure 2 with particle radii of $R_+ = R_- = 250$ nm. The stability ratios for heteroaggregation $W^{(a)}$, and the inverse collision efficiencies for deposition $W^{(d)}$, are presented. For the deposition, the same size of particles was used as for the heteroaggregation, while the collector radius is taken as $R_C = 0.1$ mm. In Figure 2, the charge density of the first particle is fixed, while the surface charge density of the second particle or of the collector is varied. Figure 2a shows the similarly charged system, which corresponds to homoaggregation or to deposition of charged particles to similarly charged substrate. These situations were studied experimentally and theoretically earlier.[12,18,21,51,52] At low salt concentrations, the system is stable, and the stability ratio is high. At higher concentrations, the stability ratio rapidly decreases and reaches unity at higher concentrations. The latter part is referred to as the fast or diffusion controlled regime, whereas the former as the slow or reaction controlled regime. The sharp transition between these two regimes is referred to as the CCC. The boundary conditions have only a minor influence on the results. The stability curves for heteroaggregation and deposition are very similar.

When the surface charge density of the second surface is lowered to $\sigma_- = 0.5$ and 0.1 mC/m^2, the CCCs shift to lower values; see Figures 2b,c. By lowering the charge of the second surface, the sensitivity on the boundary conditions increases, for heteroaggregation and deposition. Large differences in the CCC are observed for the CC, CR, and CP conditions, and the slope of the stability curve in the slow regime decreases when going from CC to CP.

In the charged-neutral case, a CCC is observed for the CC and CR conditions, whereas the CP behavior is qualitatively different; see Figure 2d. In the latter case, the stability ratio decreases monotonically with decreasing salt concentration. This behavior can be explained by the increase of the double layer attraction. Again, differences between heteroaggregation and deposition are minor.

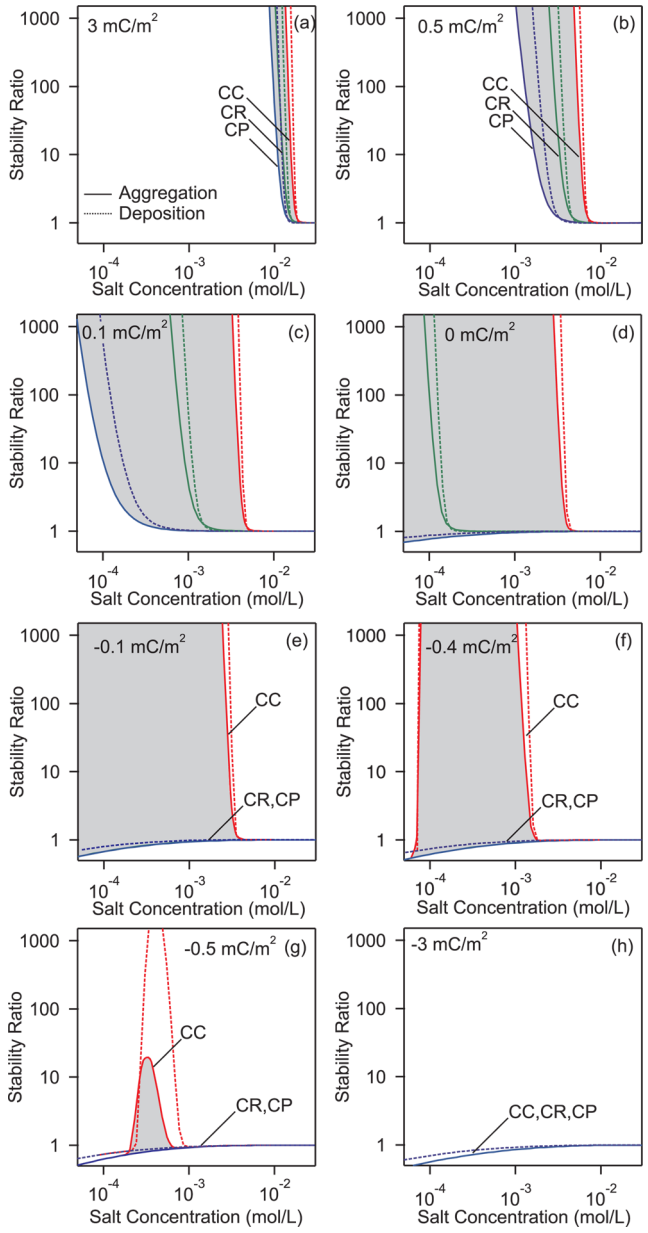

Figure 2. Stability ratios $W^{(a)}$ (full lines) and inverse collision deposition efficiencies $W^{(d)}$ (dashed lines) of differently charged colloidal particles as a function of the salt concentration of 1:1 electrolyte predicted by the DLVO theory. The PB model with CC, CP, and CR boundary conditions was used. For heteroaggregation, the first particle has a constant surface charge density of $\sigma_+ = 3$ mC/m^2, while the surface charge density of the second particle σ_- changes: (a) 3 mC/m^2, (b) 0.5 mC/m^2, (c) 0.1 mC/m^2, (d) 0 mC/m^2, (e) −0.1 mC/m^2, (f) −0.4 mC/m^2, (g) −0.5 mC/m^2, and (h) −3 mC/m^2. The Hamaker constant is $H = 5 \times 10^{-21}$ J, and for the CR conditions, the regulation parameters are $p_+ = p_- = 1/2$. Equal particle radii of $R_+ = R_- = 250$ nm are used throughout. In the case of deposition, the charge of the particle is fixed to $\sigma_+ = 3$ mC/m^2, while the charge of the collector σ_- is changed in the same manner as in the heteroaggregation. The radius of the depositing particle is equal to 250 nm, the collector radius is 0.1 mm, the approach velocity is equal to 1 mm/s, and a porosity of 0.4 is used.

When the sign of the charge on the surfaces is opposite, the stability ratio calculated with CP boundary conditions remains qualitatively the same; see Figure 2e–h. When the charge density of the second particle is decreased from −0.1 to −3

dx.doi.org/10.1021/jp503564p | J. Phys. Chem. B 2014, 118, 6346−6355

mC/m^2, the influence of boundary conditions decreases. For the oppositely charged system with $\sigma_- = -3$ mC/m^2, the stability ratios depend on the boundary conditions so weakly that this variation cannot be recognized on the scale of the figure. When the particles are oppositely charged but have charge densities comparable in magnitude, the forces calculated with different boundary conditions are all attractive. In this case, the heteroaggregation and deposition processes are limited by diffusion, and the rates depend only weakly on the magnitude of the force. An attraction influences heteroaggregation and deposition rates at low salt concentration only weakly, which is also in agreement with experiment.[38,41]

An interesting phenomenon is observed in Figure 2f,g, where surface charge densities of the second surface are −0.4 and −0.5 mC/m^2, respectively. A stable suspension is predicted in the intermediate concentration range for the CC and CR boundary conditions. This region is more pronounced in the case of deposition as compared to the heteroaggregation. The stability ratio is low at low salt concentration, and then a stable intermediate region develops at higher concentration, and by increasing the concentration further, the stability ratio decreases again. This reentrant behavior can be explained by inspecting the interaction energies between the surfaces. At high salt, there is no energy barrier and the rates are fast. At intermediate salt levels, the energy barrier develops, but it vanishes at low salt concentrations.

The effect of boundary conditions on the stability ratios is extremely strong near the charged-neutral case. When magnitudes of the surface charge densities are similar, however, the effect of boundary conditions is weak, regardless of whether the systems are similarly or oppositely charged.

Several additional parameters also influence the heteroaggregation and deposition rates, but their effect is not studied in detail here. These parameters include the Hamaker constant, particle radii, approach velocity to the collector, radius of the collector, and porosity. Normally, these parameters shift the transition between the fast and slow rates, but they can also enhance the dependencies of the rates on the salt concentration. For example, the increase of the Hamaker constant decreases the CCC and leads to a stronger dependence of the stability ratio on the salt concentration in the slow regime.

Figure 2 illustrates that stability ratios and inverse deposition efficiencies behave qualitatively similarly for all conditions studied. These similarities are not surprising, since both processes are governed by the same forces. The closer inspection reveals that the inverse collision efficiencies are shifted to higher salt concentrations. This effect is related to the fact that the forces are stronger for deposition. Because of this similarity, only stability ratios will be discussed in the following.

To get further insight into the effect of the charge asymmetry on suspension stabilities, stability maps were constructed. Figure 3a shows such a map, where the surface charge density of the second surface σ_- is plotted versus the resulting CCC. The surface charge density of the first particle is set to 3 mC/m^2. The results for the full PB model are presented on the left, and those of the DH approximation, on the right. For CP boundary conditions, the CCC is observed only when the sign of both surface charges is the same. For the oppositely charged particles, heteroaggregation is always fast, and there is no CCC. For the CC and CR boundary conditions, one observes a CCC, when one of the surfaces is close to neutral. Charge regulation effects become most important close to the charged-neutral

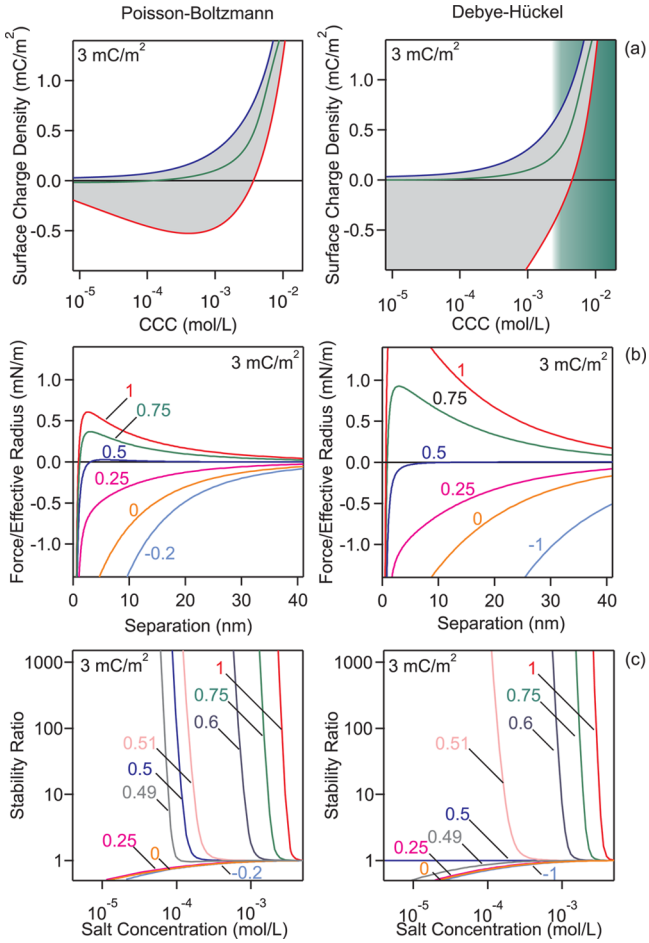

Figure 3. Effects of charge regulation on stabilities and forces in the asymmetrically charged systems in 1:1 electrolyte predicted by the DLVO theory. The surface charge density of the first particle is constant and equal to 3 mC/m^2. The PB results are presented in the left panel and the DH results in the right panel. (a) Stability map showing the surface charge density of the second particle σ_- versus the CCC. The regulation parameters for CR conditions are $p_+ = p_- = 1/2$. For DH results, the region where the surface potentials are smaller than 25 mV is shaded. (b) Forces in the *charged-neutral* system. The surface charge density of the first particle is constant, and the second particle is neutral. The regulation parameter of neutral particle p_- is varied from −1 to 1, while $p_+ = 1/2$. (c) Stability ratios in the *charged-neutral* system. The surface charge density of the first particle is constant, and the second particle is neutral. The regulation parameter of neutral particle p_- is varied from −1 to 1, while $p_+ = 1/2$. A Hamaker constant of $H = 5 \times 10^{-21}$ J and particle radii of $R_+ = R_- = 250$ nm are used throughout.

system. When the potentials are lower than about 25 mV, the PB and DH models give the same results; see Figure 3a. Another difference between the two approaches is that the DH approximation fails to predict the minimum in the stability plot for the CC boundary conditions. This minimum reflects the reentrant stability region predicted by PB theory; see Figure 2g.

Charge Regulation Effects. Charge regulation effects are important in charged-neutral systems. Let us now examine the influence of the charge regulation on forces and stability ratios.

Figure 3b shows the force profiles between a charged and a neutral particle in a 1:1 electrolyte. The surface charge density of the charged particle is 3 mC/m^2. The results of the PB model (left) and of the DH model (right) are compared. In all cases, the regulation parameter of the charged particle is fixed

dx.doi.org/10.1021/jp503564p | J. Phys. Chem. B 2014, 118, 6346−6355

to $p_+ = 0.5$, while the regulation parameter of the neutral particle p_- is varied. When this regulation parameter is varied, the forces change from attractive to repulsive. The regulation parameter of the neutral particle p_- has a very strong influence. This behavior can be understood on the DH level, since the force given in eq 11 is proportional to $2p_- - 1$. On the other hand, the regulation parameter of the charged particle influences the force only weakly. The forces calculated with PB are much lower in magnitude with respect to the DH forces. Due to the linearization inherent to the DH theory, this approximation overestimates the forces at high surface potentials.

Figure 3c shows the influence of the regulation parameter of the neutral particle on the stability ratios. The left and right panels compare the PB and DH results. The large effect of the regulation parameter on the stability ratios is also observed here. CCCs are shifting to lower values with decreasing regulation parameter. When p_- is close to zero, the suspension is no longer stabilized at lower salt concentrations, and the stability ratio decreases monotonically.

To further investigate the influence of charge regulation on the stability ratios, the shift of the CCC is plotted versus the regulation parameter in Figure 4. The relative CCCs

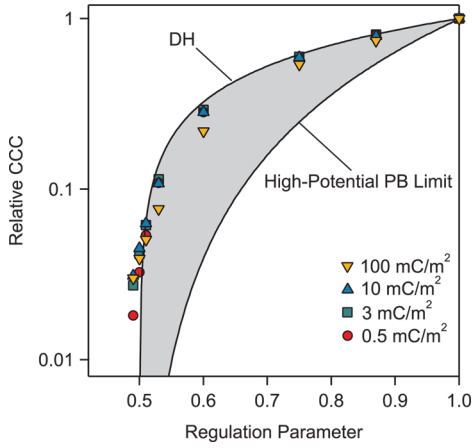

Figure 4. Relative CCC versus the regulation parameter of the neutral particle in a charged-neutral system in 1:1 electrolyte. The first particle has the charge density indicated, while the second is neutral. The CCCs are normalized to the CCC at $p_- = 1$. PB calculations are compared to analytical solution of the DH model and the hig-potential PB lmit. The regulation parameter of a charged particle is $p_+ = 1/2$. A Hamaker constant of $H = 5 \times 10^{-21}$ J and particle radii of $R_+ = R_- = 250$ nm are used.

normalized to the CCC at $p_- = 1$ are presented. The first particle is charged and its regulation parameter is fixed to $p_+ = 0.5$, while the second one is neutral and its regulation parameter p_- is varied. Symbols show the numerical PB results for different surface charge densities of the first particle, while the DH and PB limits for low and high surface charge densities are presented as lines; see eqs 18 and 19. One observes that the CCCs decrease with decreasing regulation parameter. The effect is very important, as the CCCs drop for almost 2 orders of magnitude when p_- decreases from 1 to 1/2. Within the DH approximation, the forces are always attractive for $p_- < 1/2$. In the DH limit, there are no CCCs for $p_- \leq 1/2$. For low charge densities, the results agree with this limit well. At higher surface charge densities, the PB results start to deviate. Even for high surface charge densities, however, the results do not approach the high potential PB limit. Similar behavior was found in symmetric systems, where the PB limit is only reached for unrealistically high charge densities.[21]

Multivalent Ions. Let us now discuss effects of multivalent ions on forces and stabilities for asymmetrically charged particles. In particular, we study the charged-neutral system, where the first particle is positively charged with $\sigma_+ = 3$ mC/m^2. Figure 5 presents the forces and stability ratios for three cases.

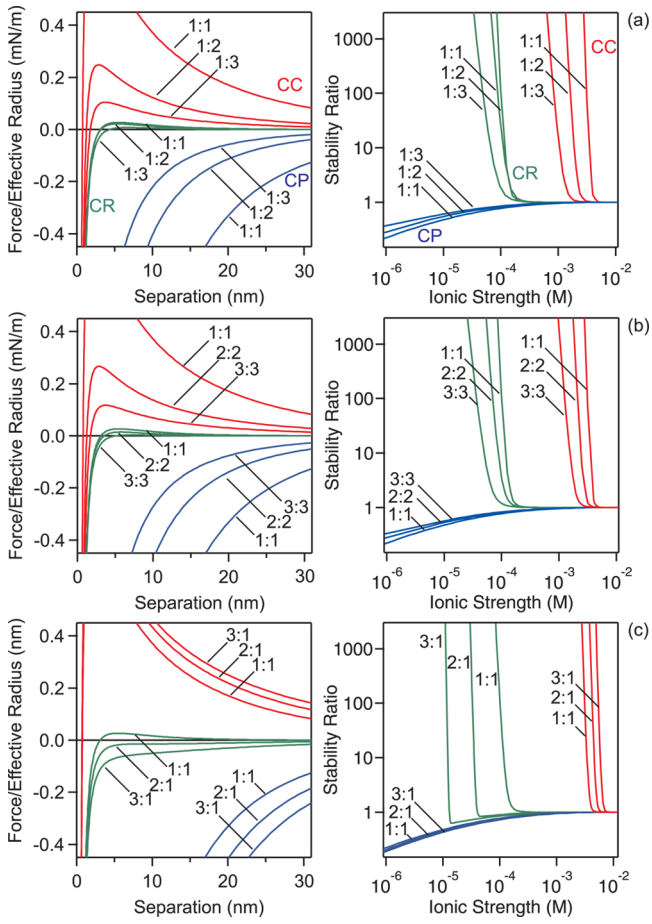

Figure 5. Interaction forces and stability ratios in the charged-neutral system in the presence of multivalent ions as predicted by the DLVO theory. The PB model with CC, CP, and CR boundary conditions is used. The surface charge density of the first particle is 3 mC/m^2, while the other particle is neutral. In the case of CR boundary conditions, $p_+ = p_- = 1/2$ is used. (a) Asymmetric 1:z electrolyte with multivalent counterions, (b) symmetric z:z electrolyte, and (c) asymmetric z:1 electrolyte with multivalent co-ions.

An asymmetric 1:z electrolyte with multivalent counterions is shown in Figure 5a, the symmetric z:z electrolyte in Figure 5b, and the asymmetric z:1 electrolyte with multivalent co-ions in Figure 5c. The forces are calculated at a constant ionic strength, and the stability ratios are plotted versus the ionic strength. Recall that the DH approximation depends only on the ionic strength, and not on the nature of the electrolytes. On the other hand, the electrolyte composition enters the PB theory. The PB predictions are similar for 1:z asymmetric and z:z symmetric electrolytes, since the counterions in both types of electrolytes have the same valence. The presence of multivalent ions lowers the magnitude of the force by electrostatic screening. Accordingly, the CCCs decrease with increasing valence for the CC and CR conditions. For CP conditions, the forces are

dx.doi.org/10.1021/jp503564p | J. Phys. Chem. B 2014, 118, 6346−6355

always attractive and no stable region results. For the CC and CR conditions, the stability ratio decreases with increasing valence. For the CP conditions, the trend is reversed; namely, the stability ratio increases with increasing valence. In the latter case, the electrostatic forces are attractive and multivalent ions are more effective in screening these forces. The case of asymmetric electrolyte with multivalent co-ions is somewhat different from the previous ones; see Figure 5c. The effect of the valence of the co-ions on the forces and stabilities is smaller, since the counterion valence is unity in all cases. For CP and CC conditions, screening of the electrostatic force is now more effective for 1:1 electrolyte as compared to the electrolytes with higher valences. In the CC case, the CCCs are shifting to higher ionic strengths with increasing valence of the co-ions. A similar trend was also observed in the case of symmetrically charged particles.[21] For CR conditions, however, screening of the electrostatic forces is more effective with increasing valence z, which is similar to 1:z and z:z electrolytes.

Further insight into the influence of the multivalent ions on the stability is gained by studying the dependence of the CCCs on the valence. Similarly to symmetrically charged particles, the DH approximation predicts that the critical coagulation ionic strength, which is the ionic strength corresponding to the CCC, is independent of the valence.[21] For the symmetric z:z electrolyte, the CCC scales as in this case as $1/z^2$; see eq 18. On the other hand, the PB equation in the high potential limit leads to the $1/z^6$ scaling relation; see eq 19.

Figure 6 summarizes relative CCCs for asymmetrically charged particles calculated with the full PB equation, and compares the low and high potential limits. Strong dependence of the CCCs on the valence is observed. Figure 6a shows the influence of the type of electrolyte. The CC conditions are used in the left column, while CR conditions with $p_- = p_+ = 1/2$, in the right column. In the CC case, PB yields a similar dependence of the relative CCCs on the ion valence for the 1:z and z:z electrolytes; see Figure 6a, left. In these cases, the dependence is stronger than what one would expect in the DH limit, whereas, for the z:1 electrolyte, the dependence is weaker. These results are in line with symmetrically charged particles.[21] In the case where the counterion is multivalent (1:z and z:z electrolyte), the screening of the surface is more effective, while in the third case where the co-ion is multivalent and the counterion is monovalent (z:1 electrolyte), screening is less effective. When surfaces regulate their charge upon approach, the results are different; see Figure 6a, right. The trends are now reversed, as the z:1 electrolyte shows the strongest dependence followed by z:z and 1:z electrolyte. In the presence of charge regulation, the neutral particle becomes negatively charged upon approach, and therefore, the situation resembles the interaction between positively and negatively charged particles. Hence, co-ions become counterions for the other surface and vice versa. The strongest screening is now present in the z:1 case, whereby the multivalent ions are counterions for the neutral surface. The latter surface becomes negatively charged upon approach.

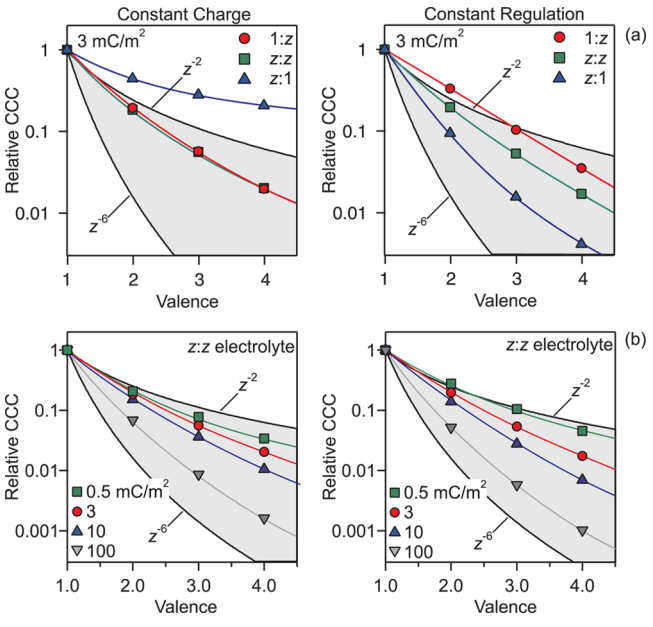

Figure 6. Relative CCC versus the ionic valence in the charged-neutral system. CCCs are normalized with respect to its value for monovalent electrolytes. The PB model with CC (left) and CR (right) boundary conditions is used. In the case of CR boundary conditions, regulation parameters are $p_+ = p_- = 1/2$. The first particle is charged, and the second is neutral. (a) Effect of the electrolyte composition, where the charge of the first particle is 3 mC/m^2. (b) Effect of the surface charge density of the first particle. The shaded area reflects the low and high potential limit.

Figure 6b shows the influence of the surface charge density of the charged particle on the CCCs in a z:z electrolyte. For the CC (left) and CR (right) conditions, the results fall inside the region between the low and high potential limits. For weakly charged particles, the results are close to the DH limit, especially in the CR case. The high potential limit is not reached even for the highest surface charge density investigated, which is similar to symmetrically charged particles.[21] Recall that the present calculations are carried out at a given surface charge density. In reality, however, the surface charge densities may vary with valence due to adsorption of these ions, and induce different z dependencies.

4. CONCLUSIONS

We have studied forces, heteroaggregation, and deposition rates involving asymmetrically charged particles and surfaces in aqueous electrolyte solutions. The interactions were described as a sum of electrostatic and van der Waals forces as summarized by the DLVO theory. The electrostatic forces were modeled at the PB level. In some cases, the DH approximation was also used for comparison. We find that, in the charged-neutral systems, where one surface is charged and the other one is neutral or close to being neutral, the forces can be either fully repulsive or fully attractive depending on the choice of the boundary conditions.

Forces between surfaces determine the heteroaggregation and deposition rates. When surfaces are similarly charged, the charge regulation effects have a rather small effect on the stabilities. Similarly, only a weak dependence of the stabilities on the regulation parameters is found in the oppositely charged systems. On the other hand, the charge regulation is extremely important in the charged-neutral case. Large shifts in the CCCs are observed for CC, CR, and CP conditions. Furthermore, even qualitative behavior may change when going from CC to CP conditions. In the charged-neutral systems, the dependence of the CCC on the regulation parameter is very strong.

In solutions containing multivalent ions, the charged-neutral systems are also highly sensitive on the valence. The CCC decreases with the square of valence for a weakly charged

dx.doi.org/10.1021/jp503564p | J. Phys. Chem. B 2014, 118, 6346−6355

surface recovering the DH limit, while with increasing surface charge the dependence is getting stronger. At the limit of extremely high charge, the Schulze−Hardy sixth power dependence is recovered; however, this limit is only achieved for surfaces with unrealistically high surface charge densities. In this respect, the charged-neutral systems behave in the same way as the similarly charged systems.

AUTHOR INFORMATION

Corresponding Author

*Phone: + 41 22 379 6054. E-mail: gregor.trefalt@unige.ch.

Notes

The authors declare no competing financial interest.

ACKNOWLEDGMENTS

This research was supported by the Swiss National Science Foundation and the University of Geneva.

REFERENCES

(1) Rasteiro, M. G.; Garcia, F. A. P.; Ferreira, P. J.; Antunes, E.; Hunkeler, D.; Wandrey, C. Flocculation by Cationic Polyelectrolytes: Relating Efficiency with Polyelectrolyte Characteristics. *J. Appl. Polym. Sci.* **2010**, *116*, 3603−3612.

(2) Horn, D.; Linhart, F. *Retention Aids*, 2nd ed.; Blackie Academic and Professional: London, 1996.

(3) Balzer, B.; Hruschka, M. K. M.; Gauckler, L. J. Coagulation Kinetics and Mechanical Behavior of Wet Alumina Green Bodies Produced Via Dcc. *J. Colloid Interface Sci.* **1999**, *216*, 379−386.

(4) Kuscer, D.; Stavber, G.; Trefalt, G.; Kosec, M. Formulation of an Aqueous Titania Suspension and Its Patterning with Ink-Jet Printing Technology. *J. Am. Ceram. Soc.* **2012**, *95*, 487−493.

(5) Trefalt, G.; Tadić, B.; Kosec, M. Formation of Colloidal Assemblies in Suspensions for $Pb(Mg_{1/3}\ Nb_{2/3})O_3$ Synthesis: Monte Carlo Simulation Study. *Soft Matter* **2011**, *7*, 5566−5577.

(6) Redman, J. A.; Grant, S. B.; Olson, T. M.; Estes, M. K. Pathogen, Filtration, Heterogeneity and the Potable Reuse of Wastewater. *Environ. Sci. Technol.* **2001**, *35*, 1798−1805.

(7) Schwuger, M. J.; Subklew, G.; Woller, N. New Alternatives for Waste Water Remediation with Complexing Surfactants. *Colloids Surf., A* **2001**, *186*, 229−242.

(8) Ryan, J. N.; Elimelech, M. Colloid Mobilization and Transport in Groundwater. *Colloids Surf., A* **1996**, *107*, 1−56.

(9) Pashley, R. M.; Israelachvili, J. N. Dlvo and Hydration Forces between Mica Surfaces in Mg^{2+}, Ca^{2+}, Sr^{2+}, and Ba^{2+} Chloride Solutions. *J. Colloid Interface Sci.* **1984**, *97*, 446−455.

(10) Kane, V.; Mulvaney, P. Double-Layer Interactions between Self-Assembled Monolayers of Ω-Mercaptoundecanoic Acid on Gold Surfaces. *Langmuir* **1998**, *14*, 3303−3311.

(11) Behrens, S. H.; Borkovec, M.; Schurtenberger, P. Aggregation in Charge-Stabilized Colloidal Suspensions Revisited. *Langmuir* **1998**, *14*, 1951−1954.

(12) Schneider, C.; Hanisch, M.; Wedel, B.; Jusufi, A.; Ballauff, M. Experimental Study of Electrostatically Stabilized Colloidal Particles: Colloidal Stability and Charge Reversal. *J. Colloid Interface Sci.* **2011**, *358*, 62−67.

(13) Ruiz-Cabello, F. J. M.; Trefalt, G.; Csendes, Z.; Sinha, P.; Oncsik, T.; Szilagyi, I.; Maroni, P.; Borkovec, M. Predicting Aggregation Rates of Colloidal Particles from Direct Force Measurements. *J. Phys. Chem. B* **2013**, *117*, 11853−11862.

(14) Sinha, P.; Szilagyi, I.; Montes Ruiz-Cabello, F. J.; Maroni, P.; Borkovec, M. Attractive Forces between Charged Colloidal Particles Induced by Multivalent Ions Revealed by Confronting Aggregation and Direct Force Measurements. *J. Phys. Chem. Lett.* **2013**, *4*, 648−652.

(15) Russel, W. B.; Saville, D. A.; Schowalter, W. R. *Colloidal Dispersions*; Cambridge University Press: Cambridge, U.K., 1989.

(16) Israelachvili, J. *Intermolecular and Surface Forces*; Academic Press: London, 1992.

(17) Ehrl, L.; Jia, Z.; Wu, H.; Lattuada, M.; Soos, M.; Morbidelli, M. Role of Counterion Association in Colloidal Stability. *Langmuir* **2009**, *25*, 2696−2702.

(18) Elimelech, M.; O'Melia, C. R. Effect of Particle Size on Collision Efficiency in the Deposition of Brownian Particles with Electrostatic Energy Barriers. *Langmuir* **1990**, *6*, 1153−1163.

(19) Ebeling, D.; van den Ende, D.; Mugele, F. Electrostatic Interaction Forces in Aqueous Salt Solutions of Variable Concentration and Valency. *Nanotechnology* **2011**, *22*, 305706.

(20) Ruiz-Cabello, F. J. M.; Maroni, P.; Borkovec, M. Direct Measurements of Forces between Different Charged Colloidal Particles and Their Prediction by the Theory of Derjaguin, Landau, Verwey, and Overbeek (Dlvo). *J. Chem. Phys.* **2013**, *138*, 234705.

(21) Trefalt, G.; Szilagyi, I.; Borkovec, M. Poisson−Boltzmann Description of Interaction Forces and Aggregation Rates Involving Charged Colloidal Particles in Asymmetric Electrolytes. *J. Colloid Interface Sci.* **2013**, *406*, 111−120.

(22) Elimelech, M.; Gregory, J.; Jia, X.; Williams, R. A. *Particle Deposition and Aggregation: Measurement, Modeling, and Simulation*; Butterworth-Heinemann Ltd.: Oxford, U.K., 1995.

(23) Carnie, S. L.; Chan, D. Y. C. Interaction Free Energy between Plates with Charge Regulation: A Linearized Model. *J. Colloid Interface Sci.* **1993**, *161*, 260−264.

(24) Behrens, S. H.; Borkovec, M. Exact Poisson-Boltzmann Solution for the Interaction of Dissimilar Charge-Regulating Surfaces. *Phys. Rev. E* **1999**, *60*, 7040−7048.

(25) Behrens, S. H.; Borkovec, M. Electrostatic Interaction of Colloidal Surfaces with Variable Charge. *J. Phys. Chem. B* **1999**, *103*, 2918−2928.

(26) Kjellander, R.; Marcelja, S. Inhomogeneous Coulomb Fluids with Image Interactions between Planar Surfaces 0.1. *J. Chem. Phys.* **1985**, *82*, 2122−2135.

(27) Forsman, J. A Simple Correlation-Corrected Poisson-Boltzmann Theory. *J. Phys. Chem. B* **2004**, *108*, 9236−9245.

(28) Trulsson, M.; Jonsson, B.; Akesson, T.; Forsman, J.; Labbez, C. Repulsion between Oppositely Charged Surfaces in Multivalent Electrolytes. *Phys. Rev. Lett.* **2006**, *97*, 068302.

(29) Bohinc, K.; Shrestha, A.; May, S. The Poisson-Helmholtz-Boltzmann Model. *Eur. Phys. J. E* **2011**, *34*, 1−10.

(30) Naji, A.; Kanduč, M.; Forsman, J.; Podgornik, R. Perspective: Coulomb Fluids—Weak Coupling, Strong Coupling, in between and Beyond. *J. Chem. Phys.* **2013**, *139*, 150901.

(31) Labbez, C.; Jonsson, B.; Pochard, I.; Nonat, A.; Cabane, B. Surface Charge Density and Electrokinetic Potential of Highly Charged Minerals: Experiments and Monte Carlo Simulations on Calcium Silicate Hydrate. *J. Phys. Chem. B* **2006**, *110*, 9219−9230.

(32) Besteman, K.; Van Eijk, K.; Lemay, S. G. Charge Inversion Accompanies DNA Condensation by Multivalent Ions. *Nat. Phys.* **2007**, *3*, 641−644.

(33) Trulsson, M.; Jonsson, B.; Akesson, T.; Forsman, J.; Labbez, C. Repulsion between Oppositely Charged Macromolecules or Particles. *Langmuir* **2007**, *23*, 11562−11569.

(34) Hatlo, M. M.; Lue, L. A Field Theory for Ions near Charged Surfaces Valid from Weak to Strong Couplings. *Soft Matter* **2009**, *5*, 125−133.

(35) Hartley, P. G.; Larson, I.; Scales, P. J. Electrokinetic and Direct Force Measurements between Silica and Mica Surfaces in Dilute Electrolyte Solutions. *Langmuir* **1997**, *13*, 2207−2214.

(36) Ruiz-Cabello, F. J. M.; Trefalt, G.; Maroni, P.; Borkovec, M. Accurate Predictions of Forces in the Presence of Multivalent Ions by Poisson-Boltzmann Theory. *Langmuir* **2014**, *30*, 4551−4555.

(37) Popa, I.; Finessi, M.; Sinha, P.; Maroni, P.; Papastavrou, G.; Borkovec, M. Importance of Charge Regulation in Attractive Double-Layer Forces between Dissimilar Surfaces. *Phys. Rev. Lett.* **2010**, *104*, 228301.

(38) Elimelech, M. Kinetics of Capture of Colloidal Particles in Packed Beds under Attractive Double Layer Interactions. *J. Colloid Interface Sci.* **1991**, *146*, 337−352.
(39) Puertas, A. M.; Fernandez-Barbero, A.; de las Nieves, F. J. Charged Colloidal Heteroaggregation Kinetics. *J. Chem. Phys.* **2001**, *114*, 591−595.
(40) Puertas, A. M.; Fernandez-Barbero, A.; de las Nieves, F. J. Induced Asymmetries in the Heteroaggregation of Oppositely Charged Colloidal Particles. *J. Colloid Interface Sci.* **2003**, *265*, 36−43.
(41) Lin, W.; Kobayashi, M.; Skarba, M.; Mu, C.; Galletto, P.; Borkovec, M. Heteroaggregation in Binary Mixtures of Oppositely Charged Colloidal Particles. *Langmuir* **2006**, *22*, 1038−1047.
(42) Hartley, P. G.; Scales, P. J. Electrostatic Properties of Polyelectrolyte Modified Surfaces Studied by Direct Force Measurement. *Langmuir* **1998**, *14*, 6948−6955.
(43) Besteman, K.; Zevenbergen, M. A. G.; Heering, H. A.; Lemay, S. G. Direct Observation of Charge Inversion by Multivalent Ions as a Universal Electrostatic Phenomenon. *Phys. Rev. Lett.* **2004**, *93*, 170802.
(44) Rentsch, S.; Siegenthaler, H.; Papastavrou, G. Diffuse Layer Properties of Thiol-Modified Gold Electrodes Probed by Direct Force Measurements. *Langmuir* **2007**, *23*, 9083−9091.
(45) Borkovec, M.; Behrens, S. H. Electrostatic Double Layer Forces in the Case of Extreme Charge Regulation. *J. Phys. Chem. B* **2008**, *112*, 10795−10799.
(46) Hogg, R.; Healy, T. W.; Fuerstenau, D. W. Mutual Coagulation of Colloidal Dispersions. *Trans. Faraday Soc.* **1966**, *62*, 1638−1649.
(47) Xu, S. H.; Sun, Z. W. Progress in Coagulation Rate Measurements of Colloidal Dispersions. *Soft Matter* **2011**, *7*, 11298−11308.
(48) Honig, E. P.; Roebersen, G. J.; Wiersema, P. H. Effect of Hydrodynamic Interaction on Coagulation Rate of Hydrophobic Colloids. *J. Colloid Interface Sci.* **1971**, *36*, 97−102.
(49) Spielman, L. A.; Friedlander, S. Role of the Electrical Double Layer in Particle Deposition by Convective Diffusion. *J. Colloid Interface Sci.* **1974**, *46*, 22−31.
(50) Elzbieciak-Wodka, M.; Popescu, M. N.; Ruiz-Cabello, F. J. M.; Trefalt, G.; Maroni, P.; Borkovec, M. Measurements of Dispersion Forces between Colloidal Latex Particles with the Atomic Force Microscope and Comparison with Lifshitz Theory. *J. Chem. Phys.* **2014**, *140*, 104906.
(51) Oncsik, T.; Trefalt, G.; Csendes, Z.; Szilágyi, I.; Borkovec, M. Aggregation of Negatively Charged Colloidal Particles in the Presence of Multivalent Cations. *Langmuir* **2014**, *30*, 733−741.
(52) Lopez-Leon, T.; Jodar-Reyes, A. B.; Bastos-Gonzalez, D.; Ortega-Vinuesa, J. L. Hofmeister Effects in the Stability and Electrophoretic Mobility of Polystyrene Latex Particles. *J. Phys. Chem. B* **2003**, *107*, 5696−5708.